In situ 7Li nuclear magnetic resonance observation of the electrochemical intercalation of lithium in graphite; 1st cycle

ARTICLE *in* CARBON · APRIL 2007

Impact Factor: 6.2 · DOI: 10.1016/j.carbon.2006.12.018

3 AUTHORS, INCLUDING:

Michel Letellier
French National Centre for Scientific Resea…
29 PUBLICATIONS **597** CITATIONS
SEE PROFILE

Mathieu Morcrette
Université de Picardie Jules Verne
143 PUBLICATIONS **5,290** CITATIONS
SEE PROFILE

Available online at www.sciencedirect.com
ScienceDirect
Carbon 45 (2007) 1025–1034
CARBON
www.elsevier.com/locate/carbon

In situ ^{7}Li nuclear magnetic resonance observation of the electrochemical intercalation of lithium in graphite; 1st cycle

M. Letellier [a,b,*], F. Chevallier [c], Mathieu Morcrette [c]

[a] CRMD, CNRS-Université, 1b rue de la Férollerie, 45071 Orléans Cedex 02, France
[b] Université François Rabelais, IUT GEII, Avenue Monge, 37200 Tours, France
[c] LCRS, Université de Picardie Jules Verne, 33 rue St Leu, 80039 Amiens Cedex, France

Received 18 March 2005; accepted 17 December 2006
Available online 27 December 2006

Abstract

We show a continuous, in situ nuclear magnetic resonance (NMR) experiment on a lithium/graphite electrochemical cell. The objective is to study a commercial graphite currently used as negative electrodes in secondary lithium batteries. A plastic cell is made, with metallic lithium as the counter electrode and 1 mol dm^{-3} $LiPF_6$/ethylene carbonate (EC) + diethylcarbonate (DEC) electrolyte. The reversible capacity is 346 mAh/g and the irreversible capacity 55 mAh/g, measured in the galvanostatic mode, at a rate of $C/20$ (20 h for the theoretical capacity of LiC_6) for the first cycle. We show the first discharge and the first charge of the cell inside the magnet and record simultaneously and regularly (in real time) static ^{7}Li NMR spectra. As expected, we observe the quadrupolar lines characteristic of the lithium graphite intercalation compounds (GICs). During the discharge, the two types of in-plane densities of Li are successively found that correspond to the dilute LiC_9, then to the dense LiC_6 configuration; during the charge, we observe the successive decrease of these states. The galvanostatic curve helps to identify the stages NMR signature and the stages coexistence.

1. Introduction

One of the many uses of graphite is as an electrode in secondary lithium batteries. The best negative electrode should be the lithium metal itself because of its low weight (0.534 g/cm^3), lowest voltage (−3.045 V for the standard Nernst voltage *vs* the normal hydrogene electrode) and high theoretical capacity (3600 mAh/g). Indeed, metallic lithium was used as first but it has the inconvenient of forming dendrites when the lithium is re-deposited on the metal during the battery charge; and this produces short-circuits.

Since the early works of Hérold and Guérard, it is known that graphite may intercalate lithium [1] by chemical route, through a staging phenomenon. By increasing the lithium concentration, the stages are $n = 4, 3, 2L$ (liquid like phase) then $n = 2$, 1 dense (composition LiC_{12}, LiC_6) at 300 K [2]. The stage number n is the number of graphene sheets between two lithium sheets.

It is also possible to intercalate lithium between the graphene sheets, by electrochemical routes [3], reversibly and with a very low voltage *vs* Li^+/Li^0, up to the stoichiometry of LiC_6, stage 1, capacity 372 mAh/g of graphite. A step by step increase of the average layer spacing d_{002} from 335 pm to 371 pm [4] is then observed for the pure stages obtained from a well ordered graphite. The advantage of using graphite instead of metallic lithium in a battery is that no dendrites are created during the charge. This has been directly evidenced by quasi in situ scanning electron microscopy [5]. When the battery is being charged, the graphite is reduced as one electron is received and, to balance the charge, one Li^+ is brought to the graphitic

* Corresponding author. Address: CRMD, CNRS-Université, 1b rue de la Férollerie, 45071 Orléans Cedex 02, France. Fax: +33 2 38 25 53 75.
E-mail address: letel@cnrs-orleans.fr (M. Letellier).

0008-6223/$ - see front matter © 2006 Elsevier Ltd. All rights reserved.
doi:10.1016/j.carbon.2006.12.018

planes, via the electrolyte, where it may nest with a charge transfer to the carbons.

Nuclear magnetic resonance is of common use to sense the chemical neighbourhood of a given nucleus but, for technical reasons, the electrochemical intercalation/disintercalation of lithium into graphite is always realized ex situ. The graphite electrode and the counter electrode are, for example, assembled in a Swagelok-type cell, and cycled in a galvanostatic mode, under constant current. When a given charge (or voltage) is achieved, the current is stopped, the cell dismantled and the graphite extracted. Some preparation is then necessary: the electrolyte and the graphite are washed in solvents and the dried powder is eventually mixed with silica and compressed into an NMR rotor for magic angle spinning. Thus, one cannot be certain that the sample still be in the electrochemical state reached in the swagelok cell. In addition, it has been shown that an improper washing of the electrode material might modify the NMR lines [6]: it seems that the reaction with the solvent tends to de-insert the lithium to form a decomposition product with a signal close to 0 ppm.

It was necessary then to allow the use of NMR for a continuous, in situ study with no destruction of the cell. Another advantage is to make possible quantitative measures on the same sample over one or several electrochemical cycles.

We did already perform in situ NMR on a disordered carbon that is more efficient than graphite [7,8], but graphite itself needed to be carefully studied since it is the most used negative electrode material in the lithium secondary batteries. Also crossing electrochemistry and NMR will certainly give a new insight into this unique property that graphite has to reversibly intercalate negative or positive ions.

Many other techniques have already been adapted to in situ situations, for example in situ X-ray diffraction [9] gives an excellent description of the swelling or shrinking of the average interlayer graphene spacing d_{002} related to lithium intercalation into graphite, or extraction. With a very slow galavanostatic rate of $C/800$, when the lithium content $x = \mathrm{Li/C_6}$ increases from 0 to 0.25, one obtains first the so-called dilute, random stage 1 (1′), then the dilute stages 4, 3, 2L with a continuously increasing d_{002} spacing corresponding to 1′ and then to the mixed phases; the coexistence of two pure phases being seen as two different spacings. From $x = 0.25$ to 0.5, one observes the coexistence of the dilute stage 2L and the dense stage 2. From $x = 0.5$ to 1 one observes the coexistence of the dense stages 2 and 1. With a faster rate ($C/40$), more than two phases can coexist at a time because the sample is not in equilibrium when the current flows [5]. In Ref. [10] the voltage is measured in open circuit conditions, when the chemical equilibrium is reached; the authors indicate four potential plateaus or semi-plateaus in the galvanostatic curve, in their Fig. 15: for $0.08 < x < 0.17$ ($220 > V > 210$ mV) coexistence of stages 8–4; for $0.17 < x < 0.33$ ($210 > V > 120$ mV) coexistence of stages 4–3–2L; for $0.33 < x < 0.5$ ($120 > V > 85$ mV) coexistence of stages 2L–2; for $0.5 < x < 1$ ($85 > V > 0$ mV) coexistence of stages 2–1. They propose an LiC_6-type for the first and second dense stages (LiC_6, LiC_{12}) and an LiC_9-type for the earlier dilute stages (LiC_{18}, LiC_{27}, LiC_{36}, LiC_{72}). Some discrepancies exist between [9] and [10] to describe and name the early stages because they are difficult to observe: does the stage 8L exist? Also the limit between the dense and dilute stages is given as $x = 0.25$ or 0.33.

To sum up, the stage 1′ ($0 < x < \sim 0.02$–0.08) is also described as a gas-like GIC, because the Li randomly occupy all the inter-layers space, and this explain the linearity between x and d_{002}. When the lithium content increases, two things occur: a 3D ordering of the graphene layers characteristic of stage formation and a densification of the lithium layer as result of gas condensation. From $x \sim 0.02$–0.08, one obtains the LiC_9-type compounds, stages 4L, 3L, 2L with a liquid-like disorder. At $x = 0.33$ the LiC_6-type compounds with a solid-like order start to grow. For $0.33 < x < 0.5$, the liquid-like stage 2L LiC_{18} and the solid-like stage 2 LiC_{12} coexist. For $0.5 < x < 1$, the solid-like stages 2 and 1 are present. At $x = 1$, all the lithium is electro-intercalated into the graphite to form the stage 1 LiC_6.

We will present here an experiment designed to follow the intercalation of lithium into graphite in real time, as it occurs when one uses a secondary battery. Actually, ^{7}Li NMR had already been performed in situ on a graphitic electrode [11], but in quite different technical conditions. The authors used a cleverly designed resonator, but the sensitivity is less than with a conventional coil, preventing a fast acquisition. Also the spectra could only be recorded in open circuit conditions: this is an advantage because one is then certain of the lithium content, but it makes it impossible to have a continuous, real-time NMR study.

2. Experimental

2.1. Graphite

We use the commercial, natural Graphite F399 from Bellcore (USA), the structure is of the hexagonal type 2H, with 15% rhombohedrical type 3R. The average crystallite parameters are: $d_{002} = 0.3354$ nm, La and Lc > 100 nm, with a maximum stacked layers size La = 500 nm. A good description of this graphite is to be found in reference [12].

2.2. Electrochemical cell

In order to study only the graphite electrode and not a complete battery, where the NMR lithium signals in the cathode would interfere, we build a battery, Fig. 1, similar to that in Refs. [7,8], with lithium metal as second electrode. Thus, the graphite becomes now the positive electrode with lithium metal as counter electrode.

We use the supple, ultra-plate plastic batteries configuration as developed by Bellcore [13]. From a powder, the graphite electrode is turned into a plastic: the graphite powder (56%) is mixed with a solution containing polyvinylidene fluoride (PVDF, binder, 16%), carbon black (SP, conductivity enhancer, 3%) and dibutyl phthalate (DBP, plasticizer, 25%) dissolved in anhydric acetone. When the graphite is plasticized, the DBP is

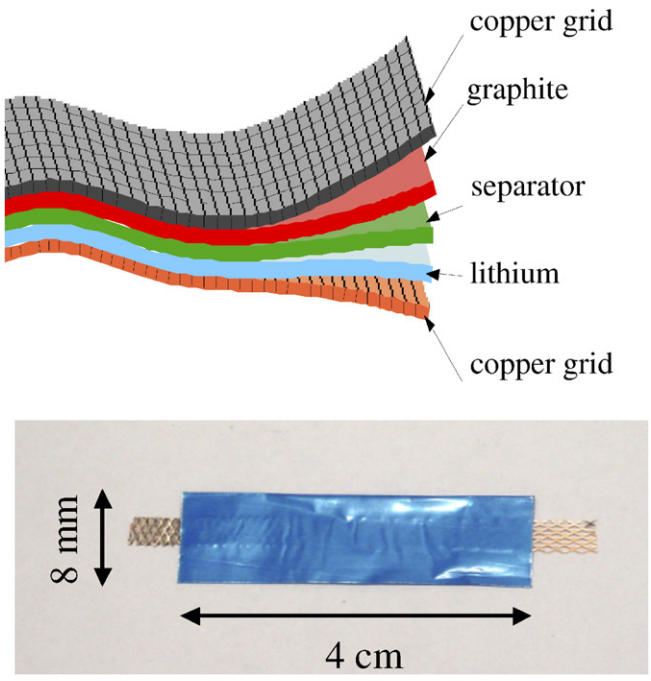

Fig. 1. Bellcore-type cell used for in situ NMR: the negative electrode is metallic lithium, the positive electrode is graphite.

removed with ether; this creates an open porosity for the electrolyte. The separator (a PVDF film containing SiO_2) is swollen by the liquid electrolyte (1 M $LiPF_6$ in a 1:1 volume ratio of ethylene carbonate EC and diethyl carbonate DEC). A foil of metallic lithium is used as counter and reference electrode. Both electrodes are pressed against rectangular copper current collectors: the dried plastic graphite film is laminated as 150 °C with the cupper grid and the separator, the lithium foil is laminated with the other cupper grid. Then both parts are laminated together and put into a blue bag that is sealed. The blue bag is made of a blue plastic covering the both sides of a thin film of aluminium, it is waterproof. The cell is assembled in an argon-filled glove box. Fig. 1 shows the NMR cell dimensions and configuration, the negative electrode being the metallic lithium foil and the positive electrode being the plasticized graphite. The graphite mass is 16.704 mg.

2.3. Battery charging and discharging

A Mac Pile generator II (BioLogic, France) is used in the galvanostatic mode to perform the electrochemical cycling. This device sinks and sources a constant current (1% stability), records the number of electrons (and counts one lithium for one electron) transferred to and from the battery and continuously measures the resulting potential (the voltage resolution is set to 5 mV). A slow ($C/20$) rate is chosen to intercalate (and dis-intercalate) one lithium in LiC_6 in 20 h with a voltage automatically ranging from 3 V to 5 mV *vs* Li^+/Li. The electrochemical cycling time is thus 40 h. Given the graphite mass, the intensity of the current is $I = 0.319$ mA. Given the graphite electrode dimensions (4×40 mm), the current density is 0.2 mA/cm^2. The $C/20$ rate was chosen for instrumental time saving, but a lower rate ($<C/40$) should be preferred to correctly distinguish all the successive GIC stages, as indicated in [4].

2.4. In situ ^{7}Li NMR

We use a 8.46 T supraconducting magnet from Oxford Instruments and a Bruker Avance DSX 360 NMR spectrometer equipped with a broadband static probe-head. The battery is fixed in a 10 mm diameter coil and the copper current collectors are welded to wires connected to the Mac Pile generator. In order to stop the high frequency noise collected by the external wires, a low pass filter is necessary on the wires. To make the sample transparent to the NMR frequencies, a thin metallic envelope is needed; that is why we use the blue bag.

The NMR settings are: frequency 139.97 MHz, single pulse sequence, sweep width 90 kHz, 80 scans, recycling time 10 s to avoid saturating a line since we expect transversal relaxation times next to 2 s for $LiPF_6$, LiC_6, and LiC_{12} [14], pulse width 5 μs. The acquisition time of one scan is 4096×5.5 μs = 23 ms. One spectrum is automatically run every hour; each acquisition lasts 13 min and we will consider we take snapshots of the system while it changes. The frequency shifts are referenced to aqueous LiCl 1 M. The temperature is 22 °C.

3. Results

3.1. Galvanostatic cycling

Fig. 2 shows the voltage V of the cell as a function of time for the first cycle.

The galvanostatic curve is exactly that of a conventional swagelok cell; we may deduce that the experimental cell is correctly fabricated and that the cycling in the NMR magnet does not affect the cell response. What is more, in our first in situ NMR study of disordered carbon [7], to make sure the intense magnetic field did not alter the cell functioning, we had cycled two identical, Bellcore cells, one in the magnet, one outside. There was only a very slight difference that could evidently result from the manufacture dispersion.

In the case of graphite, here, the plateaus under 0.22 V correspond to the coexistence of several reversible stages [9,10]. In Fig. 2 we shall name the stage-coexistence domains according to Dahn's results [9]. The voltage plateaus are best defined in [9] and at slightly higher values: 210 mV, 133 mV, 83 mV (the cycling rate was much lower and the intercalation more efficient), but our curve is very

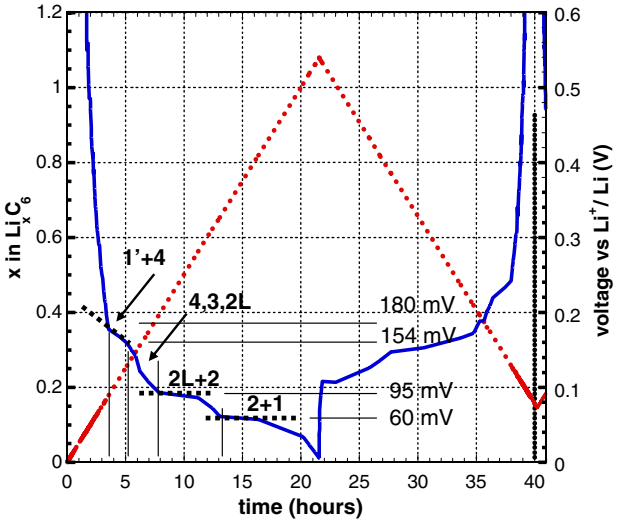

Fig. 2. First galvanostatic cycle of the Li/graphite cell: voltage (continuous line) *vs* time, the current used corresponds to a change $\Delta x = 1$ in Li_xC_6 in 20 h; the dashed line represents x. The stage-coexistences are indicated by the plateaus or semi-plateaus. The voltage transitions are given in millivolts.

similar. Here, the first intercalation lasts a little over 20 h and x exceeds 1 because some lithium are irreversibly trapped when the passivating layer (or solid electrolyte interface, SEI) is made on the graphite surface at about 0.75 V, see Fig. 3.

The frontiers between the different stages are indicated by the light, continuous, vertical lines of Fig. 2. We may then deduce which phases are present in our material as a function of the time t and as a function of the lithium content x.

For $0 < t < 3.5$ h ($0 < x < 0.18$), only stage 1′, the gas-like stage is to be found. For $3.5 < t < 5$ h ($0.18 < x < 0.24$), one should observe 1′ + 4L, liquid-like stage. For $5 < t < 8$ h ($0.24 < x < 0.4$), one should observe a mixture of the liquid-like stages 4L, 3L and 2L; for $8 < t < 13$ h ($0.4 < x < 0.65$), coexistence of 2L and the dense stage 2, for $13 < t < 21$ h ($0.65 < x < 1.078$), coexistence of the dense, solid-like stages 2 and 1. At 21.5 h, when the lithium intercalation is complete, only the dense stage 1 (LiC_6) should be found by NMR.

3.2. Galvanostatic cycling and NMR

Fig. 3 shows the first electrochemical cycle in the (x, V) coordinates with the corresponding NMR snapshots: the squares represent the average (x, V) values for each NMR spectrum. One could easily multiply the NMR spectra in order to sense almost continuously the electrochemical curve. The theoretical reversible value $x = 1$ (372 mAh/g) is reached when graphite has completely formed the first stage LiC_6. The maximum observed amount of lithium here is $x = 1.078$. It can then be measured, at the end of this first cycle, an irreversible capacity $x_{irr} = 0.1482$ (55 mAh/g) and a reversible capacity $x_{rev} = 1.078–0.1482 = 0.9298$ (346 mAh/g).

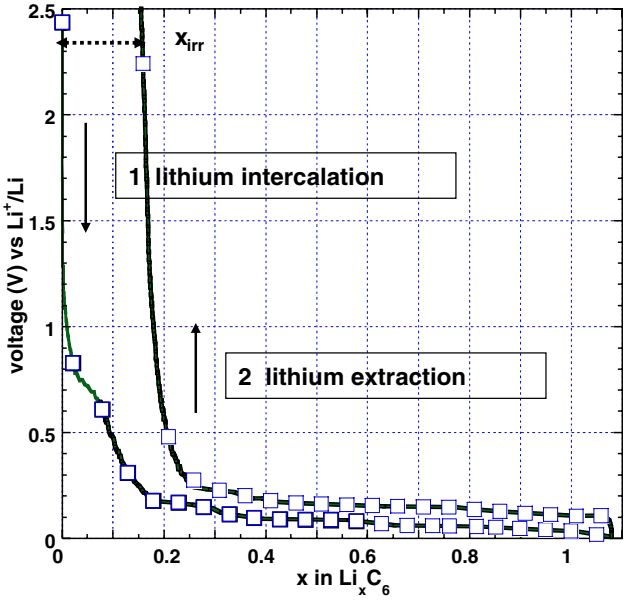

Fig. 3. First galvanostatic cycle: voltage *vs* x in Li_xC_6; the squares represent the electrochemical coordinates of the NMR spectra. The irreversible capacity x_{irr} is measured by difference between the discharge and charge curves at 3 V.

We may now synthesise the data from Figs. 2 and 3 in Table 1. We know thus at what time and x value we expect the gas, liquid, solid-like stages to occur during the first intercalation in our graphite electrode.

The corrected value $x_{corr} = x - x_{irr}$ is not exactly the actual reversible lithium amount x_{rev} all over the cycle, since the irreversible lithium is progressively trapped, but is a better approximation than the raw value x.

3.3. In situ ^{7}Li NMR spectra

Fig. 4 shows all the spectra recorded during the first lithium intercalation and extraction. The intense, Lorentzian peak at −2 ppm is that of the electrolyte $LiPF_6$. The real shape is not seen here, the magnetic field resolution being insufficient (0.3 ppm) to separate sharp peaks. The lithium irreversibly trapped in the passivating layer, most of them at the beginning of the first intercalation, give also ionic lithium signals in the 0 ppm region; they are mixed with the unresolved $LiPF_6$ signal. As time and intercalation go on, the main line to observe is near 40 ppm: its intensity increases until $x = 1.078$, then decreases; the line exhibits a pair of quadrupolar satellites (two different sizes). At the beginning of the intercalation, a smaller line is seen with a position increasing from ∼0 to 16.8 ppm. This line also possesses quadrupolar satellites of various sizes; it remains in the 16 ppm region, then shifts back to −2 ppm with the lithium extraction.

3.4. Chronology of the first intercalation seen by in situ ^{7}Li NMR

Let us now describe the chronology of the intercalation, as seen by NMR, during the first discharge ($C/20$ rate).

All the spectra show the metal line at 260 ppm, it is the lithium foil signal; this permanent signal is not displayed here.

All the spectra show the LiPF6 signal at −2 ppm. Mixed with this one are the ionic Li signals from such species as Li_2CO_3–R, $LiCO_3$–R', ... of the passivating layer around 0 ppm. We cannot, here, distinguish them and will not study them. But we demonstrate thus that the SEI NMR signals are only in the 0 ppm region.

On the very first spectra of Fig. 4 ($t < 6$ h) one sees quadrupolar satellites but no central line, because it is mixed together with the precedent lines in the 0 ppm area. We will compute the central line shift through the arithmetic mean of the satellites position, since they are symmetrical.

At 6 h 34, Fig. 5, in addition to the metal line and to the central line, only one new (quadrupolar) lithium line 1 is seen (shift $\delta 1 = 6.6$ ppm). The cell voltage being above the value (95 mV, see Fig. 2) corresponding to the beginning of the dense stage 2 (LiC_{12}), only LiC_9-type stages

Table 1
Expected Li-GIC stages to be found as a function of the time, lithium content x and corrected content $x_{corr} = x - x_{irreversible} = x - 0.1482$ (first intercalation)

t (h)	0		3.5		5		8		13		21
V (mV)	3.10^3		180		154		95		60		0
x	0		0.18		0.24		0.4		0.65		1.07
xcorr			0.032		0.092		0.25		0.5		0.93
stage		1'		1'+4L		4L+3L +2L		2L+2		2+1	

gas-like stage
liquid-like stage
solid-like stage

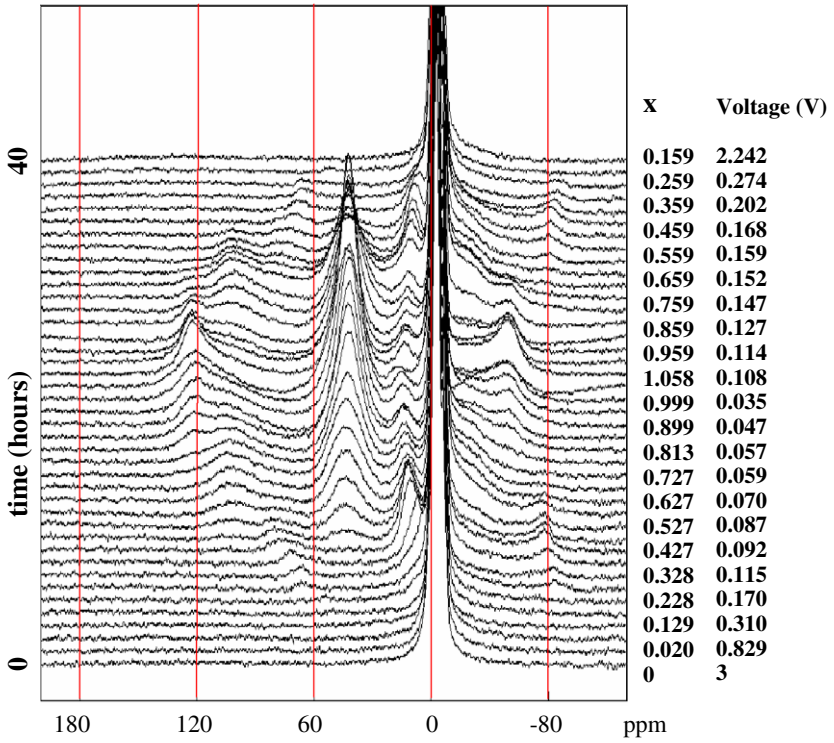

Fig. 4. In situ ^{7}Li NMR spectra for the first galvanostatic cycle: the initial spectrum ($x = 0$, $V = 3$ V) is at the bottom, then one spectrum is run each hour; every second spectrum is labelled in lithium amount $x = Li/C_6$ and voltage *vs* Li^+/Li. The horizontal axis is the NMR shift from the reference, in ppm. The vertical axis is the signal intensity; for clarity, each spectrum is offset.

are present, see Table 1. Also, the true value for x, approximated by $x_{corr} = x - x_{irr} = 0.328 - 0.1482 = 0.2798$, corresponds to the domain where the stages 4, 3, 2L may coexist, $0.17 < x < 0.33$ according to [10]. The line structure is that of a powder spectrum for a spin $I = 3/2$ sensing an axially symmetrical electrical field gradient eq ($\eta = 0$) or an axially averaged electrical gradient. The quadrupolar structure ($\nu_{Q1} = 18.4$ kHz) indicates that the lithium see a well defined electrical field gradient value with a quasi axial symmetry; if not, no quadrupolar wings should be present. This line 1 corresponds to lithium properly intercalated in the graphene layers structure and to an early, dilute stage. The quadrupolar structure (ν_{Q1}) we directly measure, as the frequency distance between the two wings of the powder spectrum, is the half of the quadrupolar momentum $Qcc = e^2qQ/h$, Q being the quadrupolar constant of ^{7}Li.

On the contrary, no quadrupolar wings were observed with disordered carbons [7]: there, the graphene layers are very short, a few nanometers wide, and many are single (wide apart) without regular stacking. When the lithium nest between the disorganized small graphene sheets, they experience each a different electrical field value, with a

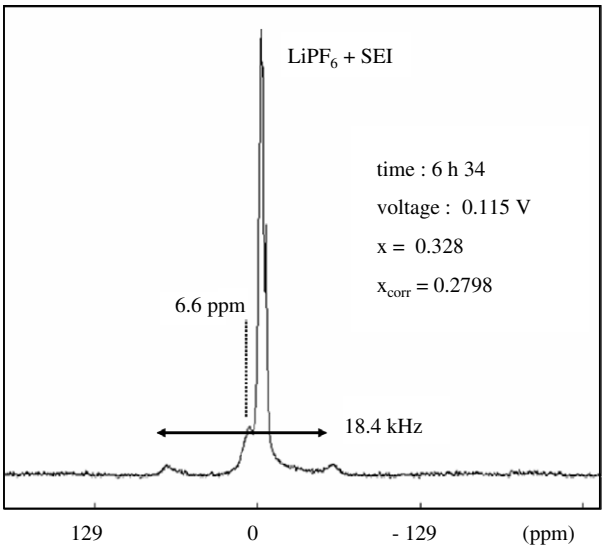

Fig. 5. NMR spectrum at 6 h 34, first discharge, $x_{corr} = x - x_{irr}$.

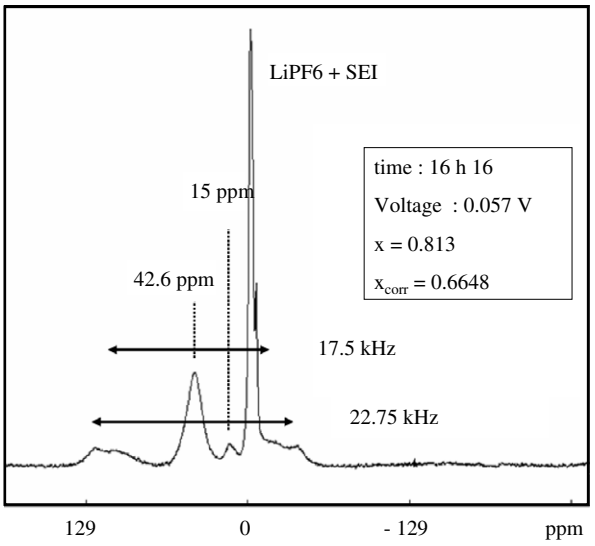

Fig. 7. NMR spectrum at 16 h 16, first discharge, $x_{corr} = x - x_{irr}$.

random orientation; thus the powder spectrum averages to zero the quadrupolar momentum.

At 9 h 32, Fig. 6, one line 1 for an intercalated dilute lithium still exists ($\delta 1 = 12$ ppm, $\nu_{Q1} = 19.2$ kHz); another line for an intercalated dense lithium is seen ($\delta 2 = 45$ ppm, $\nu_{Q2} = 16.8$ kHz): at this voltage value (89.5 mV), the dense stage 2 has begun, see Fig. 2 below 95 mV and Table 1. This last line (line 2) is the signature of LiC_{12}. Here, NMR indicates the coexistence of the dense stage 2 LiC_{12} and of a dilute stage.

At 16 h 16, Fig. 7, three lines are interesting. At this voltage, 57 mV, we expect the coexistence of the dense stages 2 and 1, see Fig. 2 between 60 and 95 mV and Table 1. Their central lines appear at the same shift (~42.6 ppm), and cannot be resolved here because of their widths. However, one may separate both lines by their quadrupolar frequencies: $\nu_{Q2} = 17.5$ kHz and $\nu_{Q2'} = 22.75$ kHz respec- tively. The unexpected line is the small line at 15 ppm. As it is small as compared to the two others, it is difficult to see if it has a quadrupolar structure. If this 15 ppm line was the continuation of the precedent 12 ppm and had a quadrupolar structure, then NMR would indicate the coexistence of three phases: LiC_6, LiC_{12} [14] and an intercalated dilute stage, that could be liquid-like or gas-like. If there is no quadrupolar structure, then the 15 ppm line could correspond to lithium inserted in a more disorganized part of the graphite, as we saw on carbon [7,8].

At 20 h 58, Fig. 8, end of the first discharge, one line corresponding to a dilute intercalated stage or to a disorganized lithium, still exists ($\delta 1 = 14.3$ ppm); its intensity is small and it is difficult to measure its quadrupolar frequency, if any.

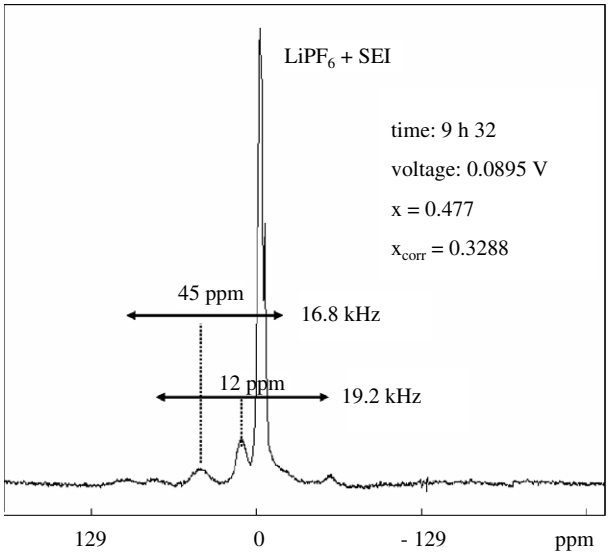

Fig. 6. NMR spectrum at 9 h 32, first discharge, $x_{corr} = x - x_{irr}$.

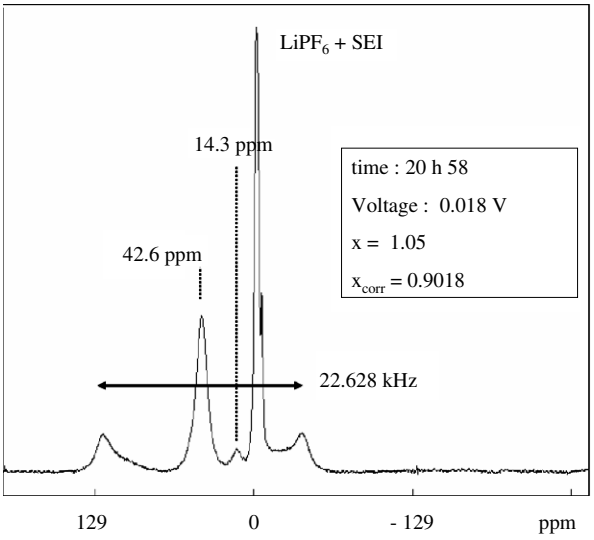

Fig. 8. NMR spectrum at 20 h 58, first discharge, $x_{corr} = x - x_{irr}$.

One single line 2 for an intercalated dense lithium is seen with $\delta 2' = 42.6$ ppm, $\nu_{Q2'} = 22.6$ kHz; it corresponds to the pure stage 1 that had already been identified in LiC_6 [14] prepared by a chemical route.

From 21.5 h to 40 h, the current is reversed and the cell charged until its voltage reaches 3 V, see Figs. 2 and 3; this corresponds to the extraction of lithium from the graphite. We observe then, see Fig. 4, the decrease in intensity of lines 2 and line 1, together with line 1 shift, in the reverse order as for the intercalation.

4. Discussion

From preceding ex situ NMR observations on a similar natural graphite by Zaghib et al. [15], it has been shown the following shifts in ppm (and quadrupolar frequency ν_Q in kHz) for stages 4, 3, 2 dilute then 2, 1 dense: 2.2 (18.4 kHz), 6.8 (18.7 kHz), 10 (19.5 kHz) then 43.8 (16.9 kHz), 41.4 ppm (23 kHz).

4.1. In situ ^{7}Li NMR data vs time

We present now all the data we may extract from the NMR spectra shown in Fig. 4. Fig. 9 summarizes the NMR data: positions $\delta 1$ (−2.6 to 16.8 ppm) and $\delta 2$ (~42 ppm) for the lines we name 1 and 2, quadrupolar frequencies ν_{Q1} (8–19.4 kHz) for line 1 and ν_{Q2} (~17 kHz) and $\nu_{Q2'}$ (~22 kHz) for line 2.

It is obvious that line 2 represents the dense stages, since it succeeds to line 1. We observe the beginning of the dense stages at 8 h $\delta 2 = 45$ ppm and $\nu_{Q2} = 17$ kHz for LiC_{12}. Then we observe the beginning of LiC_6 at 13 h: $\delta 2 \sim 42$ ppm $\nu_{Q2'} \sim 22$ kHz. At the same time the quadrupolar frequency for line 1 is no longer visible: this is consistent with the ending of the dilute stage LiC_{18} ($\delta 1 =$ 12.2 ppm, $\nu_{Q1} \sim 19$ kHz). The NMR events we see at 8 and 13 h are exactly the same as seen on the electrochemical curve in Fig. 2.

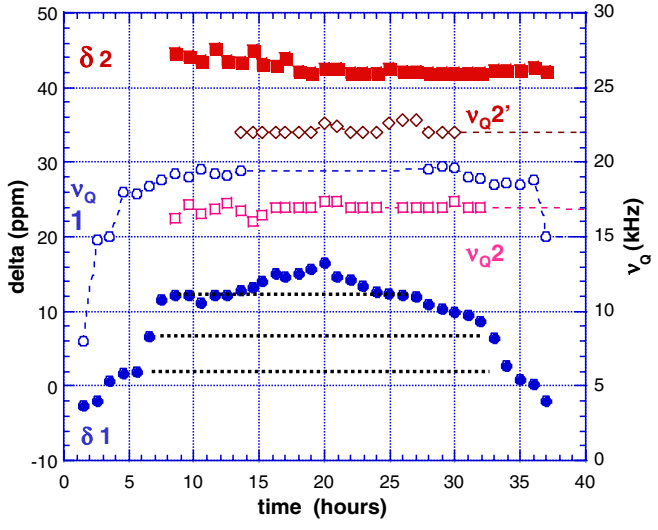

Fig. 9. First cycle, in situ ^{7}Li NMR: lines position $\delta 1$ and $\delta 2$ (respectively filled circles and filled squares), quadrupolar frequency ν_{Q1} (empty circles), quadrupolar frequencies ν_{Q2}, $\nu_{Q2'}$ of the second line (empty squares, empty lozanges), *vs* time.

From 0 to 3.5 h, we expect the random stage 1′ alone: its NMR signature is line 1, a signal ranging from $\delta 1 = -2.6$ to +1 ppm with $\nu_{Q1} = 8$–15 kHz.

For $t > 5$ h line 1 corresponds to the dilute stages 4L, 3L, 2L (LiC_9 in-plane configuration as indicated in [10]). Some discrete ($\delta 1$, ν_{Q1}) values found during the lithium intercalation seem to reappear during the lithium extraction, see the dashed lines in Fig. 9: (2 ppm, 18 kHz), (6.8 ppm, 19 kHz), (12.2 ppm, 19.4 kHz): this could indicate a given stage with an identical signature in both insertion and extraction. A possible stage 8 (1 ppm, 15 or 18.5 kHz) might also be present at about 4 and 35 h.

For $3.5 < t < 5$ h we expect the coexistence of 1′ and 4L (or 8L); one single line 1 is observed.

Concerning the reversibility of the lines in the charge part, for $21.5 < t < 40$ h, we expect a symmetrical distribution of lines 1 and 2, i.e. a symmetry of δ and ν_Q relatively to 21.5 h, when the current is reversed. We measure in Fig. 9 symmetrical $\delta 2$, ν_{Q2} for the dense stages, but not on $\delta 1$, ν_{Q1} for the dilute stages 4L, 3L, 2L. For example $\nu_{Q1} \sim 18$ kHz (for liquid-like stages) starts at 4 h ($\Delta t = 21.5 - 4 = 16.5$ h) and finishes at 36 h ($\Delta t = 36 - 21.5 = 14.5$ h). In our experiment, the dilute stage 2L starts earlier in the extraction part than in the intercalation part.

Also, due to the formation of the passivation layer, mostly during the beginning of the first intercalation, we do not know the exact composition of the graphite electrode and cannot compare directly the discharge and charge part for low contents of lithium.

4.2. In situ ^{7}Li NMR data vs x

Our experimental values for x contain the irreversible part, $x_{irr} = 0.1482$ measured at the end of the first galvanostatic cycle and we might correct x all over the curve, but this brings to negative values for very small x. Actually, the correction should be made progressively, linked to the passivation layer growing. But we do not know it. It has been reported that a battery developed an SEI all over its life, and not only during the first intercalation, so it is very difficult to be sure anyway of the real lithium content x. A very simple way to measure the lithium in the SEI (around 0 ppm) would be by in situ "liquid NMR", that is with a good magnetic field resolution.

In Fig. 10, to simplify the discussion, we only show the intercalation NMR values as a function of the experimental lithium amount x. We shall check the naming of the stages from our voltage curve, Fig. 2, according to [9,10] and Table 1. We show the three domains in x where the different gas, liquid, solid stages are expected and may thus directly identify the corresponding NMR lines.

For $0.42 < x < 1.078$, the solid-like, dense stages domain contains line 2; both shifts $\delta 2$ and $\delta 2'$ being very near, they

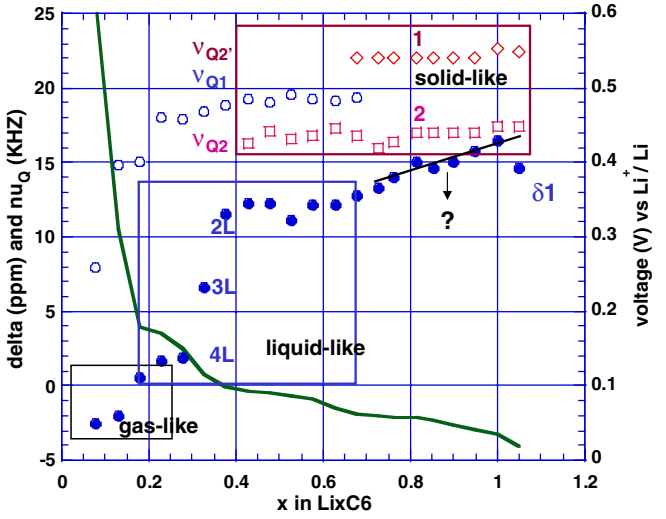

Fig. 10. Line position $\delta 1$ (filled circles) and quadrupolar frequency ν_{Q1} (empty circles), ν_{Q2} (empty squares), $\nu_{Q2'}$ (empty lozanges), as a function of $x = \mathrm{Li}/\mathrm{C}_6$; the continuous voltage curve allows to name the stage domains.

are not shown, only the quadrupolar frequencies ν_{Q2} and $\nu_{Q2'}$ appear; the values we obtain are: 45 ppm (17 kHz) for LiC_{12} and 42.6 ppm (22.6 kHz) for LiC_6, measured at $x = 1.078$. LiC_6 begins at $x = 0.65$ when ν_{Q1} finishes, exactly what was expected from the galvanostatic curve, see Fig. 2, Table 1 and exactly what is theoretically expected ($x_{rev} = 0.5$).

For $0 < x < 0.18$, the gas-like stage 1′ signature is line 1 with a shift $\delta 1 < 1$ ppm and a quadrupolar frequency $\nu_Q 1 < 15$ kHz; both seem proportional to x. This may indicate a Knight shift, as in LiC_6 [14], with $\delta 1$ proportional to the Li-2s density on the nucleus.

For $0.24 < x < 0.4$, the liquid-like signature is line 1 with $2 < \delta 1 < 12.3$ ppm and $18 < \nu_{Q1} < 19$ kHz. It seems here that each stage is characterized by $(\delta 1, \nu_{Q1})$. $\delta 1 = 2{,}6.8$, 12.2 ppm corresponds respectively to the liquid-like stages 4, 3, 2 and to the formulae LiC_{36}, LiC_{27} and LiC_{18}, see Ohzuku [10]. As a check, we may compute x_{corr} associated with the shifts 2, 6.8, 12.2 ppm, from Figs. 9 and 10. We obtain $x = 0.228$, 0.278 and 0.328 ($x_{corr} = 0.08$, 0.13 and 0.18) for the intercalation and $x = 0.409$, 0.459 and 0.509 ($x_{corr} = 0.26$, 0.31 and 0.36) for the extraction. The two parts being not symmetrical, we may estimate an average value of $x_{corr} = 0.17$, 0.22 and 0.27. This is very near the theoretical values $x = 1/6$, 1/ 4.5 and 1/3 for LiC_{36}, LiC_{27} and LiC_{18}.

For the intermediate domain $0.18 < x < 0.24$, a single line being observed; it indicates that a rapid exchange exists between the two phases.

Surprisingly, for $x > 0.65$, only solid-like stages should be present, but we still observe a line 1 shift. This would mean the coexistence of the gas-like and the solid-like phases and this is unlikely. The shift $\delta 1$ ($\nu_{Q1} = 0$) is more certainly the signature of a disordered part of the graphitic material similar to the signal we observed in disordered carbons [7,8]. It might represent lithium on the edge of the graphene layers and between graphene layers with an interlayer distance $d_{002} > 0.3354$ nm.

Another explanation might be that the cycling rate is too fast at $C/20$. One might infer that the number of lithium ions to intercalate per second is too high as compared to the diffusion ability of lithium. The in-plane diffusion rate D of lithium in graphite is not as high as other graphite intercalation compounds: $D_{LiC_6} < 10^{-12}$ m^2/s at room temperature [16]. With $D = L^2/4t$ for a bidimensional translation, one may compute, in $t = 20$ h, an average translation $L < 0.27$ mm, which is the order of magnitude of the graphite foil thickness. This might explain why all lithium have not reached the whole graphite by 20 h, but this hypothesis neglects the mobility of lithium under the influence of the applied electrical field.

4.3. In situ NMR analysis

If we compare with older results, the dense stages LiC_6 and LiC_{12}, prepared by a chemical route, were already correctly identified by ^{7}Li NMR in 1977 [14,17]. The numerous values reported in the literature for the dense stages of lithium electrochemically intercalated into graphite are also valid. Concerning the dilute stages, there is a large discrepancy in the published papers, but we found Zaghib [15] gave shift and quadrupolar momentum values quite similar to ours. Also, the ex situ values obtained by Tatsumi in [18,19] on graphite and disordered carbon are in agreement with our in situ values found here and in [7,8]. This proves that a careful electrode washing makes ex situ NMR measurements reliable.

We give, in Table 2, a comparison between our in situ NMR results and Zaghib's ex situ measurements. They are quite similar.

Table 2
Shifts δ (1 or 2) and quadrupolar structures $\nu_Q = Qcc/2$ observed for different stages by in situ NMR (here) and by Zaghib [15]

Stage	Formula from [10]	δ ppm (Zaghib)	δ ppm (in situ)	ν_Q kHz (Zaghib)	ν_Q kHz (in situ)
4	LiC_{36}	2.2	2	18.4	18
3	LiC_{27}	6.8	6.8	18.7	18.5
2	LiC_{18}	10	12.2	19.5	19
2 dense	LiC_{12}	43.8	45	16.9	17
1 dense	LiC_6	41.4	42.6	23	22.6

We observe different lines for different stages (liquid and solid-like). This indicates a relative slow diffusion between the lithium sites in the Daumas–Hérold domains of the coexisting 2L-2 and 2-1 stages.

Only for the gas- and liquid-like stages coexistence regions we observe one single line with a shift $\delta 1$. It indicates a rapid exchange (<5 μs) between stage $1'$ (shift changing) and 4L, 3L, 2L stages (fixed shift values). Thus, one may expect $\delta 1$ to depend on the respective proportion of $1'$ and 4L, 3L, 2L and on the cycling rate. This might explain why the dilute lithium position appears variable in the literature.

A tentative description of the lithium electrochemical intercalation as seen by NMR (Fig. 10) could be: the gas-like stage $1'$ forms first, with an increasing shift $d = kx$. After condensation, when the first liquid-like stage 8(?) is made, the shift takes a singular value $d8 = 1$ ppm; then, from the islands of stage 8, stage $1'$ grows with $\delta 1 = d8 + k\Delta x$; then when the stage 4 is reached, the shift takes a singular value $d4 = 2$ ppm; then, from the islands of stage 4, stage $1'$ grows with $\delta 1 = d4 + k\Delta x$ until stage 3 islands are formed with a shift $d3 = 6.8$ ppm ... then stage 2 with a shift $d2 = 12.2$ ppm. From $x = 0.35$ to $x = 0.65$, $d2$ is constant near 12.2 ppm, indicating that no exchange exists, i.e. no gas-like stage is anymore present.

5. Conclusion

This first in situ, continuous, ^{7}Li NMR observation of the electrochemical intercalation of lithium in graphite has permitted to observe the successive apparition of all the known Li-GIC stages and to give the exact values of the line shifts and quadrupolar structures. The observation of one single NMR line for $x < 0.42$ and of three lines for $x > 0.42$ suggests that the lithium diffusion is fast when in stages $1'$, 4, 3, 2 diluted and slower when in stages 2, 1 dense. We are not sure to have detected a stage 8, a slower cycling would have been necessary. We could not explain the presence, at the end of the intercalation, of a line that could represent a gas-like phase or more certainly an intercalation into a badly organized part of the graphite.

Thus, two conditions could improve the in situ observation. First, we used the first cycle of lithium intercalation/extraction in graphite and we know that most of the SEI is made during the first intercalation; therefore, we are not certain of the actual exact value for the lithium content x. Second, the cycling rate ($C/20$) is a little too high and the investigated material is in an out-of-equilibrium state. May-be this explains why line 1 is present even at the end of the intercalation. With a very slow rate, one would be at least sure that all the lithium has been intercalated in the graphite ($x = 1$) and if a line 1 still exists, it represents something else.

In situ NMR in the battery domain is only at its beginning: more appropriate, but time consuming experiments shall be made in order to do as well as in situ XRD: For example, a very slow galvanostatic rate will allow to observe the GIC stages in quasi-equilibrium and to obtain very precise NMR parameters. Another NMR technique, pulsed field gradient spin echo, might be useful to measure the lithium diffusion rate at different time scales. For a use in a battery, a good macroscopic diffusion is necessary; it has to be measured at a long time scale and that necessitates very strong gradients if the diffusion constant is small.

Acknowledgement

We thank the conseil régional de la région Centre (France) for a grant to Frédéric Chevallier.

References

[1] Guérard D, Hérold A. Intercalation of lithium into graphite and other carbons. Carbon 1975;13:337–45.
[2] Kirczenov G. Staging and kinetics. In: Zabel H, Solin SA, editors. Graphite intercalation compounds I, structure and dynamics. Springer-Verlag; 1990. p. 75–6.
[3] Yazami R, Touzain P. A reversible graphite–lithium negative electrode for electrochemical generators. J Power Sources 1983;9:365–71.
[4] Dahn JR, Fong R, Spoon M J. Suppression of staging in lithium-intercalated carbon by disorder in the host. Phys Rev B 1990;42(10):6424–32.
[5] Orsini F, du Pasquier A, Beaudouin B, Tarascon JM, Trentin M, Langenhuizen N, et al. In situ scanning electron microscopy (SEM) observations of interfaces within plastic lithium batteries. J Power Sources 1998;76:19–29.
[6] Guérin K, Ménétrier M, Février-Bouvier A, Flandrois S, Simon B, Biensan P. A ^{7}Li NMR study of a hard carbon for lithium-ion rechargeable batteries. Solid State Ionics 2000;127:187–98.
[7] Letellier M, Chevallier F, Clinard C, Frackowiak E, Rouzaud JN, Béguin F, et al. The first in situ ^{7}Li nuclear magnetic resonance study of lithium insertion in hard-carbon anode materials for Li-ion batteries. J Chem Phys 2003;118(13):6038–45.
[8] Chevallier F, Letellier M, Morcrette M, Tarascon JM, Frackowiak E, Rouzaud JN, et al. In situ ^{7}Li-nuclear magnetic resonance observations of reversible lithium insertion into disordered carbons. Electrochem Solid State Lett 2003;vol 6(11):A225–8.
[9] Dahn JR. Phase diagram of Li_xC_6. Phys Rev 1991;B 44:9170–7.
[10] Ohzuku T, Iwakoshi Y, Sawai K. Formation of lithium–graphite intercalation compounds in non-aqueous electrolytes and their application as a negative electrode for a lithium ion (shuttlecock) cell. J Electrochem Soc 1993;140(9):2490–8.
[11] Gerald II GE, Sanchez J, Johnson CS, Klingler RJ, Rathke JW. In situ nuclear magnetic resonance investigations of lithium ions in carbon electrode materials using a novel detector. J Phys: Condens Matter 2001;13:8269–85.
[12] Salver-Disma F, Tarascon JM, Clinard C, Rouzaud JN. Transmission electron microscopy studies on carbon materials prepared by mechanical milling. Carbon 1999;37:1941–59.
[13] Tarascon JM, Gozdz AS, Schmutz C, Shokoohi F, Warren PC. Performance of Bellcore's plastic rechargeable Li-ion batteries. Solid State Ionics 1996;96-88:49–54.
[14] Lauginie P, Letellier M, Estrade H, Conard J, Guérard D. Studies of graphite lithium interstitial compounds by ^{7}Li NMR and EPR. In: Proceedings of the 5th London international carbon and graphite conference; Soc Chem Ind Ed 1978. p. 645–53.
[15] Zaghib K, Tatsumi K, Sawada Y, Higuchi S, Abe H, Ohsaki T. ^{7}Li-NMR of well-graphitized vapor-grown fibers and natural graphite negative electrodes of rechargeable lithium-ion batteries. J Electrochem Soc 1999;146(8):2784–93.

[16] Magerl A. Alkali GIC's. In: Zabel H, Solin SA, editors. Graphite intercalation compounds, vol. 1. Springer-Verlag; 1990. p. 228–30.
[17] Conard J, Estrade H. Résonance Magnétique Nucléaire du Lithium Interstitiel dans le Graphite. Mater Sci Eng 1977;31:173–6.
[18] Tatsumi K, Akai T, Imamura T, Zaghib K, Iwashita N, Higuchi S, et al. ^{7}Li-Nuclear magnetic resonance observation of lithium insertion into mesocarbon microbeads. J Electrochem Soc 1996;143(6):1923–30.
[19] Tatsumi K, Conard J, Nakahara M, Menu S, Lauginie P, Sawada Yand Ogumi Z. Low temperature ^{7}Li-NMR investigations on lithium inserted into carbon anodes for rechargeable lithium-ion cells. J Power Sources 1999;81–82:397–400.